Journal of Materials Chemistry A

Accepted Manuscript

ROYAL SOCIETY OF CHEMISTRY

www.rsc.org/materialsA

ARTICLE JMCA

Safer Salts for CdTe Nanocrystal Solution Processed Solar Cells: *The Dual Roles of Ligand Exchange and Grain Growth*

Received 00th January 20xx,
Accepted 00th January 20xx

DOI: 10.1039/x0xx00000x

www.rsc.org/

Troy K. Townsend,[a]† William B. Heuer,[b] Edward E. Foos,[c] Eric Kowalski,[d] Woojun Yoon[e] and Joseph G. Tischler[e]

Inorganic CdSe/CdTe nanocrystals for solid-state photovoltaic devices are typically sintered into a bulk-like material after annealing in the presence of solid cadmium chloride. As in commercial CdTe devices, this salt exposure is a key component to improve device performance by promoting grain growth. However, in contrast to vapor depositions, we demonstrate that the role of the salt treatment also involves crucial ligand removal reactions, which are a unique challenge facing nanocrystal ink depositions. After testing other salts such as CdF_2, $CdCl_2$, $CdBr_2$, CdI_2 and $Cd(NO_3)_2$ for oleate ligand removal as determined by FTIR, SEM imaging of CdTe grain growth revealed the largest grains were observed from reactions with $CdCl_2$ (142 ± 26 nm) and, to a lesser extent, $CdBr_2$ (131 ± 19 nm). These results were used to identify cadmium-free alternatives. Trimethylsilyl chloride (28.0 ± 5.1 nm), NH_4Br (75.5 ± 31 nm) and NH_4Cl (136 ± 39 nm) were also tested, demonstrating comparable ligand removal and grain growth to the cadmium halides. In order to validate these observations, heterojunction photovoltaic devices were fabricated from CdSe/CdTe nanocrystals treated with non-toxic NH_4Cl in place of the conventional $CdCl_2$. Under AM 1.5G illumination, open circuit voltages (V_{OC}), short circuit currents (J_{SC}) and efficiencies (η) of solar cells processed with evaporated Au and commercial ITO were found to be V_{OC} = 0.46 ± 0.02 V, J_{sc} = 9.27 ± 0.6 mA cm^{-2}, and η = 1.73 ± 0.24 demonstrating minimal differences in film morphology and device performance compared to those fabricated using cadmium chloride. Specific properties of the salts (solubility, reactivity, melting point and the identity of both the cation and the anion) were found to have a profound impact on grain growth and consequently device performance, suggesting the need for further investigation of additional non-toxic metal halide salts for this reaction.

Introduction

Inorganic nanocrystal inks are attractive candidates for low-cost, high efficiency solution-based electronic devices due to their unique emerging properties. Encased in an organic ligand shell, metal and semiconducting crystals can be synthesized on the nanoscale and have found applications in a wide range of solution-compatible electronic devices including photovoltaics[1-6], light emitting diodes[7, 8], capacitors[9] and transistors[10]. Compared to conventional vapor deposition methods which require high temperatures (600-1000°C) and low pressures (ALD: 10^{-2}-10^{-5} atm), (CVD: 1-10^{-14} atm), (PVD: 10^{-10} atm) and controlled atmospheres, solution processing of nanocrystal inks can be conducted under ambient conditions (1 atm, air) with low temperature annealing (< 400°C) leading to lower cost deposition and more freedoms to coat unconventional surfaces.[11, 12] Compared to bulk material films, inorganic nanocrystals also retain synthetic control over variable electronic properties such as quantum confinement effects for semiconductors and plasmonic resonance for metallic particles, along with advantageous physical properties such as increased surface areas and reduced melting temperatures.[13, 14]

Solution-based deposition methods (drop-, spin-, spray-coating and inkjet printing) can be used for low cost high through put roll-to-roll processing and deposition onto large and irregular surfaces.[12, 15] Compared to organic compounds, inorganic materials provide superior stability against heat, UV light in conjunction with high absorption coefficients, size tunable band energy levels and high conductivities; however, they are not typically solution compatible.[16] In order to build electronic devices that bridge the gap between the superior electronic properties of inorganic materials and the solution capabilities typically associated with organics, colloidal suspensions of nanoscale inorganic crystals are synthesized and dispersed in organic solvents. Following deposition, excess ligands can be removed or exchanged to affect the desired film properties.

Recent research efforts have been focused on CdTe nanocrystals for their use in solution processed photovoltaics. In bulk-form this material has reached 20.4% efficiency commercially with First Solar Company and between 3.0% and 12.4% from nanocrystal ink precursors.[17-21] The outstanding challenge facing the (3-5 nm) inorganic nanocrystals is that they must be annealed to form larger 'bulk scale' grains (100 nm – 1 μm) in order to produce working devices.

It is widely known that cadmium chloride is an essential catalyst for the formation of bulk-scale grains of vacuum deposited cadmium chalcogenides.[22] This step is integral to the commercial fabrication of photovoltaics and also to the annealing of nanocrystal films. In an attempt to address the costly and discouraging environmental health and safety concerns of using excess cadmium salts, recent reports have shown that $MgCl_2$[23] or NH_4Cl[24] can be substituted for $CdCl_2$ for the formation of sputter-coated CdTe devices. Little is known

[a] St. Mary's College of Maryland, Department of Chemistry and Biochemistry, St. Mary's City, MD 20686
[b] U.S. Naval Academy, Department of Chemistry, Annapolis, MD 21402
[c] NSWC Indian Head EOD Technology Division, Indian Head, MD 20640
[d] ASEE NREIP Intern at the U.S. Naval Research Laboratory, Washington, DC
[e] Naval Research Laboratory, Washington, DC 20375
† Corresponding Author: tktownsend@smcm.edu

Electronic Supplementary Information (ESI) available: [XPS Spectra of 400°C annealed $CdCl_2$-CdTe films]. See DOI: 10.1039/x0xx00000x

about the mechanism of the reaction between the metal chloride and the CdTe vapor; however, there is evidence for the formation of a volatile tellurium chloride that becomes reactive at elevated temperatures (300-400°C).[25-27]

In stark contrast to vacuum-based CdTe depositions, solution-based nanocrystal depositions involve inorganic nanocrystals encased in an organic ligand shell. The insulating ligands (typically long chain carboxylic acids) remain bonded to the crystal surface during the deposition in order to maintain solubility of the colloid. In each case, the native long carbon chain ligands used in the synthesis (e.g. oleate, stearate, myristate, trioctylphosphine) are exchanged with pyridine, which is more compatible with sintering reactions. Either pyridine is more volatile (boiling point of pyridine = 115°C vs. 360°C for oleic acid) and can be removed during annealing (350 – 400°C), or it decomposes into less insulating products than the native ligands. This process in effect partially "cleans" the nanocrystals, making them suitable for sintering. However, recent studies have cited that a portion of the native ligands exist on the crystals after the pyridine exchange[28] and that attempts to further remove this ligand through extended pyridine exchange reactions causes flocculation, leading to the formation of an insoluble product.[29] Because residual oleate is an insulating material but is also required to retain solution-stabilized CdTe inks, it must be removed after deposition and before annealing to avoid hydrocarbon decomposition impurities in the film.

However, several exciting studies have recently produced nanocrystal ink dispersions stabilized by small inorganic ligands via in-solution exchange using X-/L-type ligand shells (e.g. CdSe-$CdCl_2$/BuP[30] and PbS-PbI_3/NH_3CH_3),[31] a variety of inorganic metal chalcogenides (e.g. CdSe-S^{2-})[32] and Sb_2S_3-CdSe.[33] Based on these efforts, Sargent and colleagues were able to fabricate 6% efficient solar cells using ligand-exchanged CH_3NH_3I-PbS after mild heating to remove solvent residues.[3] Due to the large Bohr radius of PbS (~20 nm) compared to ~7 nm for CdTe, sintering reactions are not necessary for efficient interparticle electronic communication. Although these efforts are promising, more work is needed to establish a link between exchange reactions and the ligand/salt-promoted sintering process required for CdTe nanocrystal solar cells – and other nanocrystal film materials aided by sintering. In an effort to shed light on the solid-state $CdCl_2$/CdTe treatment legacy and the interaction between this salt and the nanocrystal film, we monitored post-deposition small inorganic ligand exchange reactions in addition to effects on nanocrystal sintering.

This work demonstrates that the pre-annealing salt treatment is a key component for (1) catalyzing the sintering reaction between nanocrystals as observed for vacuum based deposition but also *(2) facilitating crucial ligand exchange reactions needed for the replacement of the organic ligand with an inorganic salt*. Cadmium chloride has been used previously as an initiator of the sintering reaction for CdTe nanocrystal films; however, little is known about the mechanism. In this study, we bring to light the dual role of the salt treatment and introduce the effects of changing the identity of the cation and anion. Based on the results found here, an effective salt must [1] be soluble in an organic solvent compatible with the departing ligand, [2] contain an appropriate cation for exchange reactions and [3] contain the appropriate anion to promote the sintering reaction. By elucidating the role of the salt components we were able to propose additional non-toxic salts as alternatives to $CdCl_2$.

Results and Discussion

Photo-active CdTe and CdSe films are prepared from a solution of nanocrystals, incased in long chain carboxylate ligands, by a solution deposition process (spin-, spray-, drop-, or dip-coating), as depicted in Scheme 1. In order to maintain colloidal suspensions in organic solvents, as-prepared CdTe nanocrystals typically contain insulating oleic (OA) or myristic acid (MA) ligands (Scheme 1 Stage I). These molecules, however, are not suitable for high quality film formation because they interfere with interparticle electronic interactions, forming grain boundaries and recombination sites.

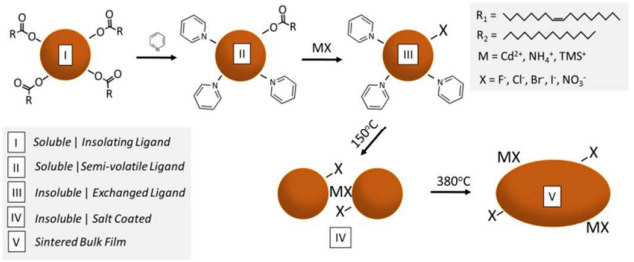

Scheme 1. Synthesis of bulk-scale CdTe films from solution soluble nanocrystal precursors including identity of the tested organic and inorganic anionic ligands with metal cations. In stage I, CdTe nanocrystals are synthesized with carboxylate ligands, where R is derived from oleic acid or myristic acid. In stage II, the nanocrystals undergo a partial ligand exchange with volatile pyridine ligand and remain soluble for solution processing. After spin-, spray-, drop-, or dip-- coating from solution, dried nanocrystal films in stage III are exposed to a salt treatment to remove residual ligands (see ionic salts above where non-ionic electrophile TMS^+ is derived from trimethylsilyl chloride). After this, they are heated at 150°C to remove volatile ligands (stage IV) and annealed at 380°C to form bulk-scale grains (stage V).

However, the long-chain ligands are crucial to the solution processing step and must remain after the partial pyridine exchange (Scheme 1 Stage II). Because this ligand interferes with the electronic properties of the film, it must be removed after film deposition and before annealing in order to avoid thermal decomposition impurities of residual organic material (oleic acid decomposes at 200°C). Since the first solution processing of CdTe / CdSe nanocrystals by Alivisatos et al. 2005, these nanocrystals have been treated with cadmium chloride in order to mimic the vacuum thin film deposition process for commercial CdTe photovoltaics.[34]

In addition to promoting nanocrystal annealing, this salt treatment provides the crucial step of complete ligand exchange. By dipping the partially exchanged nanocrystal films into saturated $CdCl_2$:methanol solutions, the residual long-chain oleate ligand is completely removed and soluble in

methanol (Scheme 1 Stage III). For this reason, water itself is not suitable for this process, whereas methanol is capable of stabilizing the removed ligands. In this step, the proposed mechanism involves substituting the anionic oleate ligands with the smaller inorganic anions from the salt.[32] Concurrently, the metal cation charge-stabilizes the organic ligand (i.e. cadmium oleate is formed). At this stage (Scheme 1 Stage III), the nanocrystals are not soluble due to the loss of stabilizing ligand. As a result, this salt treatment must be implemented after deposition from solution. Once the nanocrystals are deposited as a thin film (~60 nm thick) and ligand exchanged with the salt, the sintering reaction can proceed to form high quality films of bulk scale grains (Scheme 1 Stage IV and V).

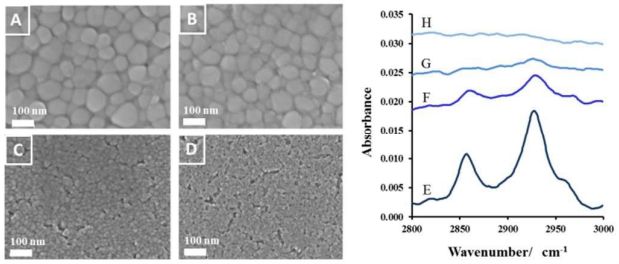

Figure 1. SEM images of 60 nm thick CdTe nanocrystal films treated with a 5 s dip in $CdCl_2$ dissolved in methanol heated to 60°C with $CdCl_2$ concentrations based on % saturation at 25°C, [A] 100% saturation, [B] 50% saturation [C], 25% saturation and [D] 12.5% saturation followed by sintering at 380°C for 25s. FTIR spectra of 60 nm thick CdTe nanocrystal films without $CdCl_2$ treatment [E], with 1 s dip [F], with 5 s dip [G] and with 30 s dip [H] in 25°C 100% saturated $CdCl_2$ in methanol heated to 60°C.

The role of complete ligand removal from the $CdCl_2$ salt treatment was revealed from SEM images of annealed CdTe nanocrystal films treated with various concentrations of $CdCl_2$ in methanol and from FTIR spectra of the as-deposited nanocrystal films after dipping in $CdCl_2$:methanol (Figure 1). The concentration of salt in the methanol solution plays an important role in the degree of sintering as shown in Figure 1A-D. Thin films of pyridine-exchanged CdTe nanocrystals were spin-coated and dipped into 100%, 50%, 25% and 12.5% saturated $CdCl_2$:methanol solutions heated to 60°C. After annealing at 380°C for 25 s, the resulting films produced larger grains when treated with more concentrated $CdCl_2$ solutions. More available $CdCl_2$ in solution was able to complete ligand exchange and coat the surface of the nanocrystals with the salt. In agreement with this, FTIR spectra showed that longer soaking times from 0 s to 30 s dip in $CdCl_2$:methanol were directly related to a systematic removal of oleic acid as measured by the disappearance of the C-H alkyl stretching bands at 2924 and 2852 cm^{-1} from non-treated (Figure 1E) to a 30s dip treatment (Figure 1H). In cases where the pyridine exchanged CdTe films were treated with a drop-coat of $CdCl_2$ in methanol, grain growth was only partially observed and the resulting film after annealing revealed blended grains without clear crystallites as was reported by others.[35] Without the salt-induced ligand removal process, the oleate ligands remain, leading to insulating organic decomposition products. For this reason, a simple drop-coating of $CdCl_{2\ (s)}$ will not lead to significant grain growth during annealing. Early devices by Carter et al. used the drop-coating of $CdCl_2$-methanol during spin-coating; however, this would also lead to ligand exchange as the methanol solution is removed during the spinning process.[17]

With the goal of ligand exchange in mind, myristic acid (MA) (saturated 14 carbon chain) was tested in place of unsaturated 18 carbon oleic acid (OA). Myristic acid has previously been hypothesized to promote faster CdTe oxidation due to a more accessible nanocrystal surface resulting from the straight carbon chains.[36] This is in contrast to unsaturated chains (like oleic acid capped crystals, which show slower oxidation in air). Because this physical difference may also apply to attack by pyridine molecules through the ligand layer, thus allowing the pyridine molecules to more easily reach the nanocrystal surface to remove long chain ligands, myristic acid capped CdTe nanocrystals were also synthesized in an attempt to achieve complete pyridine exchange. However, after the pyridine treatment, these crystals also contained residual myristate (Figure 2h).

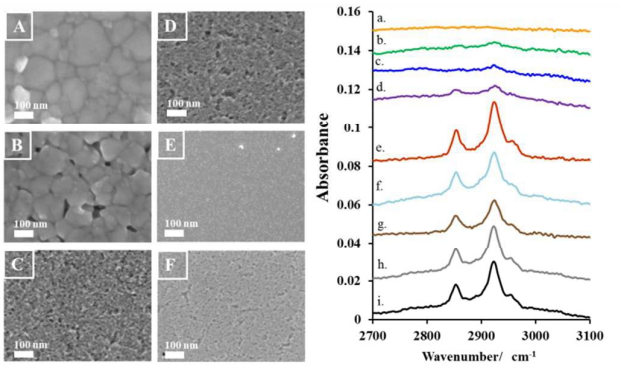

Figure 2. SEM images of 60 nm thick CdTe nanocrystal films treated with 25°C 100% saturated salts solutions in methanol heated to 60°C followed by sintering at 380°C for 25s – ordered according to grain size with [A] $CdCl_2$, [B] $CdBr_2$, [C] CdI_2, [D] $Cd(NO_3)_2$, [E] CdF_2 and [F] methanol only. Included are the corresponding FTIR spectra of (A-F) CdTe films after salt treatment but before annealing for [a] $CdCl_2$, [b] $CdBr_2$, [c] CdI_2, [d] $Cd(NO_3)_2$, [e] CdF_2 and [f] methanol only. Pre-salt treated CdTe nanocrystal films are shown after [g] pyridine exchange of OA-capped crystals, [h] pyridine exchange of MA-capped crystals and [i] as synthesized OA-capped crystals.

The salt treatment, however, provided complete removal of the oleate ligands and therefore; alternative salts to cadmium chloride were tested for their efficiency for both ligand removal and grain growth. In order to test the effect of different anions in the cadmium series, we exposed the CdTe films to CdX_2:methanol solutions were X = F, Cl, Br, I and nitrate (Figure 2). After annealing, substantial grain growth was observed for crystals treated with $CdCl_2$ (142 ± 26 nm) and $CdBr_2$ (131 ± 19 nm), whereas the other treatments did not yield sintering (Figure 2, A-F). In order to gain insight into the differences between these reactions, FTIR spectra were taken after treatment with CdX_2 salts (Figure 2 a-e), after methanol soaking (Figure 2 f) and on the as-deposited films (Figure 2 g-i). Pure methanol was tested as a control to eliminate the possibility that the oleate ligands would spontaneously dissociate into solution in the absence of the salt.

The CdF_2 treatment did not yield grain growth and the FTIR spectra show no ligand exchange. Cadmium fluoride was found to be insoluble in methanol and therefore was not able to complete the ligand exchange reaction in solution. In contrast, the other salts were soluble in methanol and demonstrated effective oleate removal, with the exception of $Cd(NO_3)_2$ which showed partial exchange. Both CdI_2 and $Cd(NO_3)_2$ did not yield grain growth upon heating, which may be explained by the reactivity of the anion (discussion later).

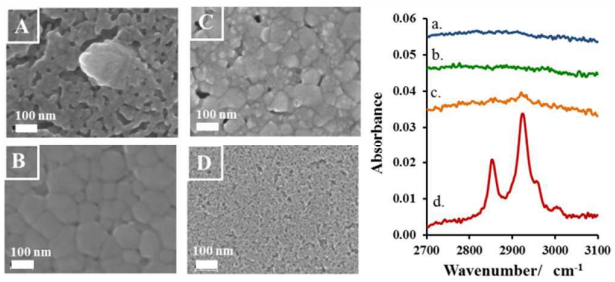

Figure 3. SEM images of 60 nm thick CdTe nanocrystal films treated with 25°C salt solutions heated to 60°C of [A] 1 mL TMSCl in 20 mL acetonitrile or saturated in methanol for [B] NH_4Cl, [C], NH_4Br, and [D] methanol only, followed by sintering at 380°C for 25s. Included are corresponding FTIR spectra of salt treated CdTe nanocrystal films (A-D) before annealing [a, b, c and d], respectively.

Based on this, the identity of the anion plays an important role in ligand removal and the grain growth process. Likewise, the identity of the cation also contributes to the annealing products. In order to test the effects of various cations, the anions from the previous successful cadmium salts (chloride and bromide) were paired with alternative cations of ammonium and a non-ionic Lewis acid, trimethylsilyl (TMS) group. Surprisingly, ammonium chloride and ammonium bromide demonstrated significant grain growth to an extent comparable to their cadmium halide counterparts. Figure 3 A-D shows the SEMs of CdTe films annealed after salt treatment. The methanol control did not show grain growth; however, NH_4Cl produced large grains (136 ± 39 nm), NH_4Br showed moderately large grains (75.5 ± 31 nm) and TMSCl yielded grain growth to a smaller extent (28.0 ± 5.1 nm). Likewise, the FTIR spectra of pre-annealed CdTe films treated with these salts dissolved in methanol revealed that each of these three alternative salts effectively removed oleate ligands (Figure 3 a-d).

Reasons for minimal grain growth with TMSCl may be related to the reactivity of this compound with water and alcohol. In theory, Me_3Si-Cl reacts with the carboxylate ligand to form a silyl ester, leaving behind a chloride on the surface of the nanocrystals. This is supported by the FTIR spectra showing complete removal of the carboxylate ligand. However, grain growth was not observed despite the presence of chloride. The film processing involves exposure to isopropanol and water vapor from the air, and TMS-Cl readily hydrolyses to form hexamethyldisiloxane and HCl. The presence of the siloxane impurities would interfere with grain growth, and excess H^+ from HCl was found to dissolve the CdTe film without producing grain growth during our preliminary studies.

The effects of the salts tested in this study as they apply to both ligand removal and grain growth are summarized in Table 1. Using Beer's Law, proportional oleate ligand concentrations were calculated from the 2924 cm^{-1} absorbance peak heights as a percentage of exchange relative to the as-prepared starting material after pyridine treatment. In cases where the salt was not soluble in methanol, grain growth either did not proceed, or was limited as observed for cadmium fluoride and trimethylsilyl chloride. In the case of cadmium nitrate, this salt was soluble in methanol; however, the exchange reaction was incomplete (73%) and this may have influenced the lack of observed grain growth. In other cases, salts were both soluble and effectively removed ligands; however, they still did not yield large grains. This was true for cadmium iodide (83%), where the properties of the large iodide anion drastically influenced the sintering reaction. The trend improves with smaller halide anions where salts with bromide yielded medium sized grains and chloride containing salts produced the largest grains.

Table 1. Summary of the properties and effects of the salts tested in this study on 60 nm films of 3-5 nm CdTe nanocrystals before sintering and the resulting grain growth after a 25 s heat treatment at 380°C to promote grain growth.

Salt	Methanol Solubility	Proposed Leaving Group	Exchanged Anion	Exchange (%)	Grain Size (nm)
$CdCl_2$	High	Cadmium Oleate	Cl^-	100	142 ± 26
NH_4Cl	High	Ammonium Oleate	Cl^-	100	136 ± 39
$CdBr_2$	High	Cadmium Oleate	Br^-	85	131 ± 19
NH_4Br	High	Ammonium Oleate	Br^-	84	75.5 ± 31
TMS-Cl	N/A*	TMS-Oleate	Cl^-	100	28.0 ± 5.1
CdI_2	High	Cadmium Oleate	I^-	83	7.06 ± 1.6
Methanol	N/A	None	None	0	6.43 ± 1.0
$Cd(NO_3)_2$	High	Cadmium Oleate	NO_3^-	73	5.7 ± 1.0
CdF_2	Very Low	Cadmium Oleate	F^-	0	4.93 ± 1.8

* Trimethylsilyl chloride (TMS-Cl) was dissolved in acetonitrile because it decomposes rapidly in methanol

The relative sizes of the I^-, Br^- and Cl^- anions could play a role in the permeability of these ions through the film, leaving deeper nanocrystal surfaces untouched by the salt. However, each of these cadmium salts demonstrated reasonable ligand exchanges (83, 85 and 100%, respectively) suggesting efficient anion permeation despite the differences in atomic size, although there is a slight trend favoring smaller anions. Additionally, self-ionization of neutral metal halides in polar solvents is well-known, leading to coordinated complexes of Cd^{2+}, CdX^+, CdX_2, CdX_3^- and CdX_4^{2-}. Here, the majority species depends on the nanocrystal surface affinity for anionic ligands and the properties of the solvent (Lewis character and ability to stabilize cations and anions).[31] This may account for differences in ionic permeability and ligand exchange effectiveness among the cadmium halides. This is also reflected in the increasing aqueous pKsp values: $CdCl_2$(0.68) < $CdBr_2$(2.42) < CdF_2(2.98) < CdI_2(3.61).[37] Separately, $Cd(NO_3)_2$ is very soluble in polar solvents due to the weakly coordinating NO_3^- anion. However, this would also explain why $Cd(NO_3)_2$ was less effective at displacing the native oleate ligands.

Beyond ligand exchange, the second crucial reaction involves chemical sintering. Therefore, ineffective salts either do not form the correct sintering intermediates or are not reactive at the sintering temperature. According to reports on commercial vacuum deposited CdTe, the presence of volatile $TeCl_{2\ (g)}$ is observed as an intermediate product of the reaction between CdTe and $CdCl_2$ as described in the sequence shown in Equations 1 and 2 as it applies to CdTe nanocrystal sintering.[26, 38, 39]

$$CdTe_{nano\ (s)} + CdCl_{2\ (s)} + \frac{1}{2}O_{2\ (g)} \rightarrow Cd_{(s,l)} + CdO_{(s)} + TeCl_{2(l,g)} \qquad Eq.1$$

$$TeCl_{2(l,g)} + 2\ Cd_{(s,l)} \rightarrow CdTe_{bulk\ (s)} + CdCl_{2\ (s)} \qquad Eq.2$$

The thermal properties of $TeCl_2$ ($T_{melting}$ = 208°C, $T_{boiling}$ = 328°C) match well with the annealing temperatures typically used to sinter CdTe nanocrystals (350-400°C).[12, 19] In this case, $TeCl_2$ vaporizes during the sintering process, promoting a sintering reaction with local CdTe nanocrystals. As the 3-5 nm nanocrystals react with the tellurium halide, the sintering reaction proceeds through a break-down of small crystallites and reforming of bulk-scale crystal grains. This process relies on the formation of CdO and $TeCl_2$ which promote mobility of Cd and Te atoms at the grain boundaries during nano-CdTe recrystallization.[38] It is not surprising that the optimal sintering temperature for these nanocrystals was found to be 380°C[12], which is close to the boiling point of the $TeCl_2$ intermediate. Therefore, the grain-growth effectiveness of the cadmium halide is most likely a direct result of the reactivity of the tellurium halide intermediate at the sintering temperature.

Table 2. Physical properties of tellurium halides (MP = melting point, BP = boiling point, D. = decomposes, Subl. = sublimes at 25°C[40, 41]

Salt	MP(°C)	BP(°C)
TeF_2	*	*
$TeCl_2$	208	328
$TeBr_2$	210	339
TeI_2	Subl.	*
TeF_4	129	195
$TeCl_4$	224	380
$TeBr_4$	380	420
TeI_4	280	D.
$Te(NO_3)_2$	D. (190-300°C)	

* Data not available

Evidence for this arises from the slightly lower effectiveness of cadmium bromide, which forms $TeBr_2$ ($T_{melting}$ = 210°C, $T_{boiling}$ = 339°C) and is more thermally stable than $TeCl_2$. This salt vaporizes at the sintering temperature of 380°C; however, the reaction may not proceed as readily, producing smaller CdTe grains (Figure 2B). Little is known about the properties of CdI_2, (Table 2 suggests that it is unstable above room temperature) although following the physical trends ($T_{boiling}$ $TeCl_2$ = 328°C < $T_{boiling}$ $TeBr_2$ = 339°C), this salt is expected to produce a tellurium (II) iodide intermediate with even higher melting and boiling temperatures (Table 2), leading to no grain growth at 380°C as observed in Figure 2C. This suggests that sintering with CdI_2 would require higher temperatures than for $CdCl_2$ to produce larger CdTe grain sizes, and likewise for each halide, more experiments would be required to determine their optimal annealing temperatures. Cadmium nitrate on the other hand, would not be capable of forming a tellurium halide, which may eliminate nitrate as a possible anion for this reaction. Nitrates would also favor the oxidation of CdTe, leading to insulating oxides of Cd_xTe_yO.[26] In addition, $Te(NO_3)_2$ decomposes below 200°C, which also renders it unsuitable as an intermediate for CdTe recrystallization, as we have not observed grain growth below this temperature for any salt. Consequently, $Cd(NO_3)_2$ did not lead to grain growth (Figure 2D). The formation of tellurium tetrahalides (TeX_4, where X = F, Cl, Br, I) are also possible, although the boiling points of these are typically higher than the dihalides and less likely to proceed (Table 2).

In addition, considering possible Cd:Te ratio changes that occur during ligand exchange reactions as reported for some solution phase dispersions (i.e. initial Cd:Te > final Cd:Te due to loss of Cd-oleate),[30] the amounts of sintering reactants may vary among the halide salt treatments. Solution processed CdTe/Se nanocrystals have been shown to contain an excess of Cd^{2+},[30] and changes in this concentration could impact the annealing process or p/n doping. Future work in our lab involves quantifying these changes for various salt treatments; however, initial XPS data on 380°C $CdCl_2$ annealed CdTe nanocrystal films is given in Figure S1 and Table S1. Interestingly, more O (68% higher) and more Cd were found on the surface (Cd:Te = 1.57) than subsurface (Cd:Te = 1.10). This is in very close agreement with to atomic compositions found for 400°C annealed $CdCl_2$-CdTe films prepared by standard chemical bath deposition as reported by Niles et al. Here, surface Cd concentrations (Cd:Te = 1.96) were also higher than subsurface Cd (Cd:Te = 1.12) along with 75% more surface O.[27] As proposed in their study, Te^{2-} converts to Te^{4+} in the presence of oxygen. This points to the formation of a $TeOCl_2$ or $TeCl_4$ intermediate along with a surface Cd-O species, which contributes to excess surface Cd. Likewise, our Te 3d spectra also contain both oxidation states of Te after annealing nano-CdTe in air. Compared to pre-annealed CdTe, Niles et al. also observed a drop in Te and Cl concentrations after annealing further supporting the presence of a volatile Te-halide intermediate.[27]

Unlike the cadmium salts, ammonium chloride is unique such that any excess decomposes during annealing ($T_{melting}$ = 338°C) into NH_3 and HCl gas. Since this process occurs below the annealing temperature for nano-CdTe, the effects of residual cation in the CdTe film are minimal. However, this may not be true for other metal chlorides (such as $CdCl_2$ and $MgCl_2$).[23, 42]

Based on these results, the chlorides were shown to produce the most effective sintering due to their efficiency of oleate ligand removal paired with enhanced reactivity with CdTe nanocrystals due to higher volatility of tellurium intermediates. The identity of the cation is also important, although the change from cadmium (II) to ammonium was not as pronounced as the change among the halides.

Table 3. Summary of performance of solution processed heterojunction solar cells (ITO/CdSe/CdTe/Au) in the dark and under AM 1.5G filtered spectral illumination (100 mW cm^{-2}) including shunt resistivity (Rsh) of the devices shown in Figure 4B, averaging data from 10 devices for each treatment. The device area is 0.1 cm^2.

Treatment	Voc (V)	Jsc (mA cm^{-2})	FF (%)	Rsh (Ω cm^2)	Efficiency (%)
1. CdSe ($CdCl_2$) / CdTe ($CdCl_2$)	0.52 ± 0.02	9.42 ± 3.2	43.3 ± 2.9	(4.1±2.1) x 10^3	2.37 ± 0.23
2. CdSe ($CdCl_2$) / CdTe (NH_4Cl)	0.47 ± 0.02	9.37 ± 0.8	43.3 ± 1.3	(1.1±4.2) x 10^4	1.91 ± 0.23
3. CdSe (NH_4Cl) / CdTe (NH_4Cl)	0.46 ± 0.02	9.27 ± 0.6	40.1 ± 2.1	(2.9±1.5) x 10^3	1.73 ± 0.24

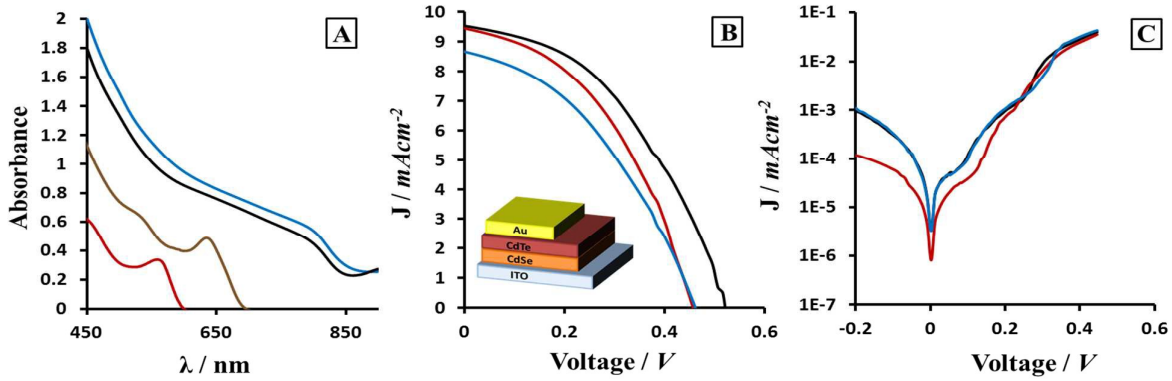

Figure 4. UV Vis absorbance spectra [A] of oleate-capped CdSe (red) and CdTe (brown) nanocrystals in solution and CdSe/CdTe heterojunction films on ITO after sintering with $CdCl_2$ (black) and NH_4Cl (blue). [B and C] Light and dark I-V curves, respectively of heterojunction (ITO/CdSe/CdTe/Au) solar cells under 1 sun simulated sunlight, device area is 0.1 cm^2, constructed from nanocrystals treated with $CdCl_2$ as a control for both CdTe and CdSe (black), NH_4Cl treatment for CdTe / $CdCl_2$ for CdSe (red), and NH_4Cl treatment for both CdSe and CdTe (blue) see Table 3 for more device parameters.

For this reason, ammonium chloride shared properties with cadmium chloride, and the resulting grain sizes were comparable, suggesting that ammonium chloride should be a suitable alternative.

In order to test this, solar cells with the device structure glass/ITO/CdSe/CdTe/Au were fabricated and treated with ammonium chloride in place of cadmium chloride. The photovoltaic responses of these devices under simulated one sun are summarized in Table 3. Here, films of nanocrystals (3-5 nm) of CdSe (60 nm thick) and CdTe (500-600 nm thick) were spin coated onto ITO/glass and treated with either cadmium chloride or ammonium chloride. Using the established method with $CdCl_2$ for both layers[20], the devices produced a larger voltage (0.52±0.02 V) compared to the devices prepared with NH_4Cl for both layers (0.46±0.02 V). Because the voltages in these heterojunction devices are based on the band energetics between the two semiconductors, the annealing parameters can greatly impact the device properties. Small changes in annealing temperature and heating time can lead to large variation in the open circuit voltages and short circuit currents of these nanocrystal films because of the sensitive nature of device processing leading to reported Jsc values ranging from 0.7 to 25 $mAcm^{-1}$.[12, 19, 42] Therefore, the optimal annealing parameters for $CdCl_2$ treated nanocrystals would not necessarily be identical for those treated with ammonium chloride or other metal halides. For this reason, the devices prepared with NH_4Cl demonstrated slightly lower efficiencies (η = 1.73±0.24) compared to $CdCl_2$ devices (η = 2.37±0.23) and CdSe($CdCl_2$)/CdTe(NH_4Cl) with intermediate efficiencies (η = 1.91±0.23). However, these differences are minimal and are expected to improve after further optimization of the ammonium halide systems.

Figure 4A shows the UV/Vis absorption spectra of CdSe and CdTe nanocrystals prior to annealing and CdSe/CdTe devices after annealing at 380°C for 25 s in the presence of $CdCl_2$ or NH_4Cl salts. During heating, the nanocrystals form larger bulk-scale crystal grains (λ = 810 nm) from quantum confined CdSe (λ = 555 nm) and CdTe (λ = 638 nm). Both salts produce optically similar films as supported by the grain growth observed in the SEM images (Figure 2,3). Figure 4B gives the current-voltage curves for devices 1, 2 and 3 from Table 2 under simulated sunlight and in the dark. All three device performances were similar and the effect of switching to ammonium salts did not drastically affect the device properties.

Conclusions

Solution processed CdTe nanocrystal photovoltaics typically require a sintering step to form large bulk-scale grains with enhanced film properties. Despite the importance of this step, little is known about the mechanism of the salt-nanocrystal interactions. For the first time, the salt treatment was found to remove residual long-chain organic ligands used during synthesis. These ligands are insolating and their decomposition products inhibit the formation of high quality semiconductor films. The photo-electronic properties of these films are

improved after the replacement of the oleate ligand for a smaller inorganic anion. The identity of the cation is important as well, as it should act as a counter ion for the leaving anionic ligand. After testing the effects of cadmium halides (F^-, Cl^-, Br^- and I^-), $Cd(NO_3)_2$, trimethylsilylchloride and ammonium halides (Cl^- and Br^-) for both ligand removal and grain growth effectiveness, it was concluded that the salt must meet specific criteria in order to be a viable alternative to $CdCl_2$. These include: [1] the salt must be soluble in organic solvent in order to provide a medium for the leaving anionic organic ligand, [2] it must contain the appropriate cation in order to complete the ligand exchange reaction and alleviate the anion for the sintering process and [3] an appropriate anion is required based on the reactivity of the sintering intermediates where smaller halide anions form more reactive intermediates leading to larger grain growth. Assuming these criteria are followed, alternative salts for sintering nanocrystals may be identified. Here, we demonstrate for the first time that ammonium chloride is a non-toxic, inexpensive viable alternative to cadmium chloride for nanocrystal solar cells. Devices made using ammonium chloride had comparable device characteristics to those made with cadmium chloride. These results have implications for photovoltaics in addition to other electronic devices fabricated from sintered nanocrystals (PV, LEDs, transistors, capacitors, etc.). In addition, the move away from cadmium salt treatments alleviates concerns about the environmental health and safety of current processing methods. Next generation solar cells with solution-based deposition capabilities require safe handling when considering the freedom to paint or spray onto large and irregular surfaces.[12, 43] Given the criteria outlined here, organic-soluble fluoride salts should be tested for these reactions due to their potential for low boiling point tellurium salt intermediates. In addition, further optimization of the annealing parameters for NH_4Cl is needed to achieve higher efficiencies. These results may also be applicable to annealing solid-state device materials other than CdTe. Progressing away from the historical use of cadmium may yield even more enhanced film properties for nanocrystal film sintering reactions.

Materials and methods

Reagents

All reactions were conducted under inert conditions using standard Schlenk techniques unless otherwise noted. Oleic acid (90%), 1-octadecene (90%), trioctylphosphine (TOP) (90%), trimethylsilyl chloride (99.9%), Se (99.5+%), CdF_2 (99%), $CdCl_2$ (99.9%), $CdBr_2$ (98%), CdI_2 (99.9%), $Cd(NO_3)_2$ (99%), NH_4Cl (99%) and NH_4Br (99%) were purchased from Aldrich. CdO (99.99%) and Te (99.8%) were purchased from Strem. All reagents were used as received within 6 months except for pyridine which was purified through distillation.

Active layer nanocrystal synthesis

CdTe and CdSe nanocrystals were synthesized following a literature procedure.[35] Briefly, CdO (0.48 g; 3.74 mmol), oleic acid (4.29 g; 15.19 mmol) (or 3.47g ; 15.19 mmol of myristic acid) and 76 mL of 1-octadecene were combined in a 250 mL 3-neck flask. This solution was evacuated at 100°C for 20 min then filled with Ar and brought to 260°C. Tellurium (0.24 g; 1.88 mmol) or selenium (0.153 g; 19.37 mmol) powder was sonicated in TOP (4.39 g; 11.84 mmol), combined with 5 g 1-octadecene and injected into the flask after removing from heat at 260°C for CdTe or 250°C for CdSe nanocrystals. The reaction was cooled naturally to room temperature and the resulting nanocrystals were precipitated with the addition of 75 mL heptane (99%) and 150 mL ethanol (99.5%). They were re-dissolved in 5 mL pyridine and heated under Ar for 18 h at 85°C. Following this pyridine exchange, the nanocrystals were precipitated in 40 mL hexanes (95%) to remove excess ligands and re-dissolved in a 5 mL pyridine–5 mL 1-propanol (99.5%) mixture to produce 40 mg mL^{-1} CdTe and 16 mg mL^{-1} CdSe nanocrystal stock solutions.

Device fabrication and salt treatment

Devices were built on commercially available indium-tin oxide (ITO, 8–12 $\Omega\ \square^{-1}$ Delta Technologies) coated glass substrate (25 mm by 25 mm by 1.1 mm) which were first sonicated in acetone and ethanol and blown dry using N_2. Using tape to mask strips, ITO substrates were etched in a 10% aqueous aqua regia solution set at 60°C until the glass was exposed to produce patterned ITO of 0.318 cm strips to allow for the construction of multiple devices on each substrate. These substrates were then cleaned with ethanol followed by brief 3 s dip in 10% by volume aqua regia at room temperature and rinsing with water. Drops of silver epoxy were painted onto the edge of the ITO electrodes (outside of the PV device area) and annealed at 380°C to insure direct contact with the ITO anode prior to device fabrication. This was found to be necessary due to the difficulty of scratching the active layers to expose the ITO for ohmic contact after CdSe/CdTe annealing. The active layers were then deposited starting with CdSe (16 mg mL^{-1}) and followed by CdTe (40 mg mL^{-1}). These nanocrystal stock solutions were spin coated at 850 rpm for 30 s onto the ITO substrate and dried at 150°C for 1 min to remove solvent. After cooling to room temperature, the nanocrystal film was dipped in a 25°C saturated $CdCl_2$–MeOH solution (99% MeOH) heated to 60°C, then immediately dipped into iPrOH (99%) to remove excess $CdCl_2$ and blown dry with N_2. The film of nanocrystals (3–5 nm) was placed on a hot plate at 380°C for 25 s to induce sintering and form larger grains (50–200 nm). After cooling to room temperature, the film was rinsed in water to remove excess $CdCl_2$. Alternative salt substitutions were used at the same concentration in methanol by weight of 70 mg salt in 40 mL methanol. This process was repeated iteratively to build the CdSe and CdTe films layer-by-layer to reach the desired thicknesses of each material, typically 3 layers for 60 nm thick CdSe and 6 layers for 400 nm thick CdTe. Devices were completed with thermally evaporated gold contacts with an Edwards Auto 306. The samples were pumped under vacuum to ~10^{-7} Torr and using a shadow mask, 140 nm Au was deposited onto the CdTe

surface. Each type of gold contact was masked to form 0.318 cm wide strips orthogonal to the patterned ITO to ultimately produce 10 square devices per 6.25 cm^2 substrate each with an area of 0.10 cm^2.

Characterization and device testing

Film morphology, thickness and surface roughness were determined with a Leo 1550 SEM and a Zygo optical profilometer. Grain sizes were measured with ImageJ software. X-ray photoelectron spectra were taken with a Thermo Scientific K-alpha XPS equipped with Ar sputter depth profiling. The current density–voltage characteristics of the photovoltaic devices were measured with an Oriel PVIV-1A Test Station where solar cell efficiency was measured under the spectral output from a 150 W solar simulator (Newport) using an air mass 1.5 global (AM 1.5G) filter. The irradiance (100 mW cm^{-2}) of the solar simulator was adjusted using a reference cell 91150V (Newport) traceable to the National Renewable Energy Laboratory (NREL). Shunt resistivities were calculated from the slope of the dark current IV curves and series resistivities were determined from the multi-light method. Sheet resistances and resistivities of the contacts were calculated from a four point probe measurement.

Acknowledgements

The Office of Naval Research (ONR) is gratefully acknowledged for financial support. This work was conducted while Professor Townsend held a National Research Council (NRC) Postdoctoral Fellowship at the Naval Research Laboratory. E.K. acknowledges the Naval Research Enterprise Internship Program (NREIP).

Notes and references

1 R. Debnath, O. Bakr and E. H. Sargent, *Energy & Environmental Science*, 2011, **4**, 4870-4881.
2 J. Tang and E. H. Sargent, *Advanced Materials*, 2011, **23**, 12-29.
3 Z. Ning, H. Dong, Q. Zhang, O. Voznyy and E. H. Sargent, *ACS Nano*, 2014, **8**, 10321-10327.
4 W. Yoon, J. E. Boercker, M. P. Lumb, D. Placencia, E. E. Foos and J. G. Tischler, *Scientific Reports* 2013, **3**.
5 Z. Jiaoyan, Y. Yuehua, G. Yuping, Q. Donghuan, W. Hongbin, H. Lintao and H. Wenbo, *Nanotechnology*, 2014, **25**, 365203.
6 B. Zhao, Z. He, X. Cheng, D. Qin, M. Yun, M. Wang, X. Huang, J. Wu, H. Wu and Y. Cao, *Journal of Materials Chemistry C*, 2014, **2**, 5077-5082.
7 Y. Shirasaki, G. J. Supran, M. G. Bawendi and V. Bulovic, *Nat Photon*, 2013, **7**, 13-23.
8 H. V. Demir, S. Nizamoglu, T. Erdem, E. Mutlugun, N. Gaponik and A. Eychmüller, *Nano Today*, 2011, **6**, 632-647.
9 G. Yu, L. Hu, M. Vosgueritchian, H. Wang, X. Xie, J. R. McDonough, X. Cui, Y. Cui and Z. Bao, *Nano Letters*, 2011, **11**, 2905-2911.
10 B. A. Ridley, B. Nivi and J. M. Jacobson, *Science* (New York, N.Y.), 1999, **286**, 746-749.
11 S. E. Habas, H. A. S. Platt, M. F. A. M. van Hest and D. S. Ginley, *Chemical Reviews*, 2010, **110**, 6571-6594.
12 T. K. Townsend, W. Yoon, E. E. Foos and J. G. Tischler, *ACS Applied Materials & Interfaces*, 2014, **6**, 7902-7909.
13 A. N. Goldstein, C. M. Echer and A. P. Alivisatos, *Science* 1992, **256**, 1425-1427.
14 P. Buffat and J. P. Borel, *Physical Review A*, 1976, **13**, 2287-2298.
15 K. Zweibel, *Solar Energy Materials and Solar Cells*, 1999, **59**, 1-18.
16 C. J. Brabec, *Solar Energy Materials and Solar Cells*, 2004, **83**, 273-292.
17 T. Ju, L. Yang and S. Carter, *Journal of Applied Physics*, 2010, **107**, 104311.
18 B. I. MacDonald, A. Martucci, S. Rubanov, S. E. Watkins, P. Mulvaney and J. J. Jasieniak, *ACS Nano*, 2012, **6**, 5995-6004.
19 M. G. Panthani, J. M. Kurley, R. W. Crisp, T. C. Dietz, T. Ezzyat, J. M. Luther and D. V. Talapin, *Nano Letters*, 2013, DOI: 10.1021/nl403912w.
20 W. Yoon, T. K. Townsend, M. P. Lumb, J. G. Tischler and E. E. Foos, *Nanotechnology, IEEE Transactions on*, 2014, 1.
21 H. Liu, Y. Tian, Y. Zhang, K. Gao, K. Lu, R. Wu, D. Qin, H. Wu, Z. Peng, L. Hou and W. Huang, *Journal of Materials Chemistry C*, 2015, DOI: 10.1039/C4TC02816C.
22 S. A. Ringel, A. W. Smith, M. H. MacDougal and A. Rohatgi, *Journal of Applied Physics*, 1991, **70**, 881-889.
23 J. D. Major, R. E. Treharne, L. J. Phillips and K. Durose, *Nature*, 2014, **511**, 334-337.
24 J. D. Major, L. Bowen, R. E. Treharne, L. J. Phillips and K. Durose, *Photovoltaics, IEEE Journal of*, 2015, **5**, 386-389.
25 M. Terheggen, H. Heinrich, G. Kostorz, A. Romeo and A. Tiwari, Munich, Germany, 2002.
26 US 6,251,701 B1, 2001.
27 D. W. Niles, D. Waters and D. Rose, *Applied Surface Science*, 1998, **136**, 221-229.
28 J.-K. Lee, M. Kuno and M. G. Bawendi, *MRS Online Proceedings Library*, 1996, **452**, 1-5.
29 I. Lokteva, N. Radychev, F. Witt, H. Borchert, J. r. Parisi and J. Kolny-Olesiak, *The Journal of Physical Chemistry C*, 2010, **114**, 12784-12791.
30 N. C. Anderson and J. S. Owen, *Chemistry of Materials*, 2013, **25**, 69-76.
31 D. N. Dirin, S. Dreyfuss, M. I. Bodnarchuk, G. Nedelcu, P. Papagiorgis, G. Itskos and M. V. Kovalenko, *Journal of the American Chemical Society*, 2014, **136**, 6550-6553.
32 A. Nag, M. V. Kovalenko, J.-S. Lee, W. Liu, B. Spokoyny and D. V. Talapin, *Journal of the American Chemical Society*, 2011, **133**, 10612-10620.
33 J. J. Buckley, M. J. Greaney and R. L. Brutchey, *Chemistry of Materials*, 2014, **26**, 6311-6317.
34 I. Gur, N. A. Fromer, M. L. Geier and A. P. Alivisatos, *Science*, 2005, **310**, 462-465.
35 J. Jasieniak, B. I. MacDonald, S. E. Watkins and P. Mulvaney, *Nano Letters*, 2011, **11**, 2856-2864.
36 S. Sun, H. Liu, Y. Gao, D. Qin and J. Chen, *Journal of Materials Chemistry*, 2012, **22**, 19207-19212.
37 J. W. Ball and D. K. Nordstrom, WATEQ4F -- User's manual with revised thermodynamic data base and test cases for calculating speciation of major, trace and redox elements in natural waters, Report 90-129, 1991.
38 G. S. Khrypunov, *Semiconductors*, 2005, **39**, 1224-1228.
39 N. Romeo, A. Bosio, R. Tedeschi and V. Canevari, *Materials Chemistry and Physics*, 2000, **66**, 201-206.
40 M. J. d. Exter, Immobilisation of Iodine, 2004.
41 D. R. Lide, CRC Handbook of Chemistry and Physics, 88th edn., 2008.
42 A. Bezryadina, C. France, R. Graham, L. Yang, S. A. Carter and G. B. Alers, *Applied Physics Letters*, 2012, **100**, 013508.
43 T. K. Townsend and E. E. Foos, *Physical Chemistry Chemical Physics*, 2014, **16**, 16458-16464.

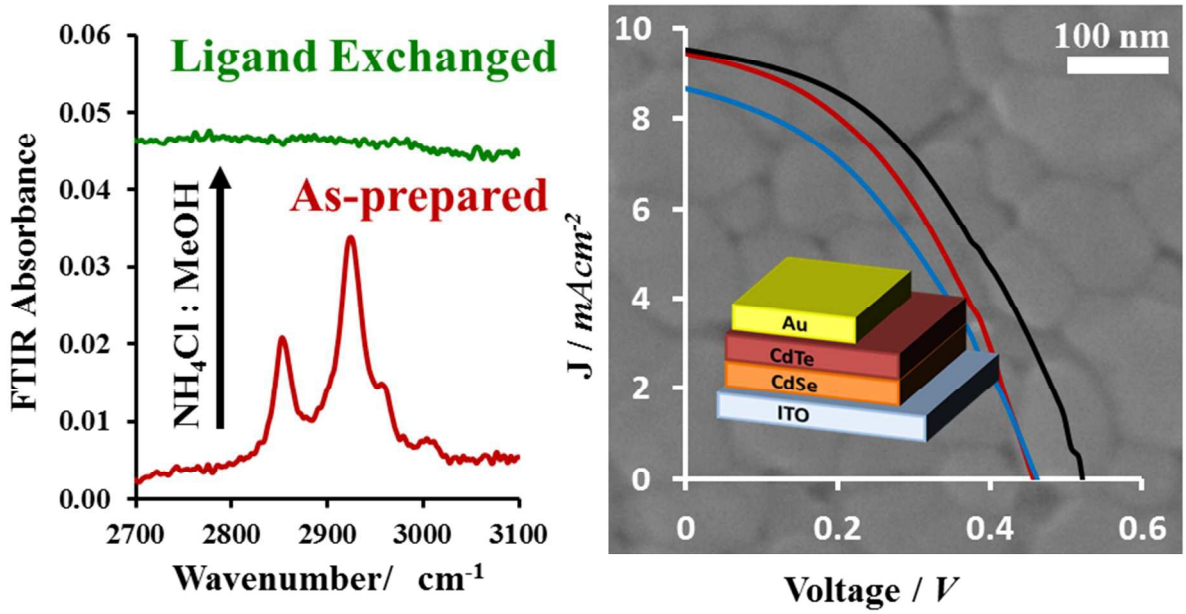

The dual role of salt treatment was revealed by replacing conventional $CdCl_2$ with non-toxic NH_4Cl to simultaneously exchange native ligands and promote grain growth in inorganic CdTe nanocrystal solar cells.